ELSEVIER

Journal of Alloys and Compounds 1 (2002) 000–000

Journal of ALLOYS AND COMPOUNDS

www.elsevier.com/locate/jallcom

XAS spectra of $Ce_2[MnN_3]$ at the Ce-$M_{4,5}$, Ce-L_3, Mn-$L_{2,3}$ and N-K thresholds

R. Niewa[a,*], Z. Hu[b], C. Grazioli[b], U. Rößler[b], M.S. Golden[b], M. Knupfer[b], J. Fink[b], H. Giefers[c], G. Wortmann[c], F.M.F. de Groot[d], F.J. DiSalvo[e]

[a]*Max-Planck-Institut für Chemische Physik fester Stoffe, Nöthnitzer Str. 40, 01187 Dresden, Germany*
[b]*Institut für Festkörper- und Werkstofforschung Dresden, P.O. Box 270016, 01171 Dresden, Germany*
[c]*Fachbereich 6-Physik, Universität Paderborn, 33095 Paderborn, Germany*
[d]*Solid State Physics, University of Groningen, Nijenborgh 4, 9747 AG Groningen, The Netherlands*
[e]*Department of Chemistry, Cornell University, Ithaca, NY 14853-1301, USA*

Received 5 November 2001; received in revised form 29 March 2002; accepted 29 March 2002

Abstract

The X-ray absorption spectroscopy at the Ce-$M_{4,5}$, Ce-L_3, Mn-$L_{2,3}$ and N-K thresholds was used to study the electronic and magnetic structure of the recently obtained $Ce_2[MnN_3]$. Manganese is found to be in a state similar to that in η-Mn_3N_2, with strong covalency between Mn and N. The multiple peaked structure in the Ce-$M_{4,5}$ and Ce-L_3 XAS spectra indicates that the valence state of cerium in $Ce_2[MnN_3]$ is only slightly lower than that found in CeO_2 containing Ce^{IV} with a strong covalent mixture between Ce 4f and ligand 2p states. By simulating the Ce-L_3 XAS spectrum using a simplified Anderson impurity model the 4f occupancy was found to be 0.52 for $Ce_2[MnN_3]$ compared to 0.49 for CeO_2 in the ground state.

Keywords: Ternary nitrides; Nitridomanganates; XAS; Rare earth; Electronic state

PACS: 78.70. Dm; 71.28.+d; 79.60

1. Introduction

During the last decade, the electronic and the magnetic properties of 3d transition metal (TM) compounds have been intensively studied using the high energy spectroscopy stimulated by the discovery of high-T_c cuprates [1]. The combined theoretical and experimental studies of X-ray absorption spectroscopy (XAS) at the thresholds provide information on the electronic states of metal atoms and the distribution of the valence electrons between metal and ligand atoms [2–5]. Contrary to the valuable results on oxides and halides obtained with XAS only a small number of reports in the literature deals with nitrides, mostly on binary or quasi-binary systems. Few XAS investigations on nitridometalates have been reported [6–8]. That is partly due to the difficulties in preparation of single phase samples and handling the compounds, which are often highly sensitive to moisture. Extensive exploratory activities in recent years resulted in a number of new nitridometalates with unusual oxidation states of transition metals [9–11]. In comparison with oxide chemistry, low oxidation states seem to be preferred in nitrides, e.g. Mn^I, Fe^I, Co^I, Ni^I. In this work the Mn-$L_{2,3}$, Ce-$M_{4,5}$ and Ce-L_3 XAS spectra are used to determine the electronic states of manganese and cerium in the recently described compound $Ce_2[MnN_3]$ [12]. The three plausible assignments of oxidation states for the metals were previously proposed: $(Ce^{IV})_2[Mn^IN_3]$, $(Ce^{III})_2[Mn^{III}N_3]$, and $Ce^{IV}Ce^{III}[Mn^{II}N_3]$, provided that nitrogen is formally N^{3-} [12].

The electronic state of the metal species in such compounds is not a trivial question. Magnetic measurements do not always give a correct formulation, since even the binary cerium nitride, CeN, in which the Ce ion is close to Ce^{3+}, shows just Pauli-paramagnetism [13]. From XAS it is well known that cerium ions do not usually follow the simple notations Ce^{3+} and Ce^{4+}, but rather exhibit intermediate valence state behavior [14–16]. For example, in the cerium oxide CeO_2 the 4f occupancy n_f was found to be ~0.59 [16]. Therefore, it can be called an intermediate valence state due to the strong 4f configura-

*Corresponding author.
E-mail address: niewa@cpfs.mpg.de (R. Niewa).

0925-8388/02/$ – see front matter © 2002 Published by Elsevier Science B.V.
PII: S0925-8388(02)00519-4

8045 DTD431 29−APR−2002 10:28:56.13 v1.4.48

tion mixing known from high energy spectroscopy [16–18]. From the viewpoint of chemical bonding, one can still assign the oxidation state four to Ce^{IV} compounds, but one should bear in mind that the ground state is a mixture of Ce 4f, 5d and/or 6s atomic states with valence states of neighboring atoms, e.g. for oxides $\alpha_0 | 4f^0\rangle + \beta_0 | 4f^1\underline{L}\rangle$ ($\underline{L}$ denotes a hole at the O 2p state), in the same way as for Cu^{III} in $NaCuO_2$ and $La_2Li_{0.5}Cu_{0.5}O_4$ [2,19]. For $Ce_2[MnN_3]$ it was concluded from DFT calculations that cerium is Ce^{IV}, and in turn Mn^I [20]. The electronic and magnetic structures of manganese ions are not simple. In oxides, manganese ions usually exist in oxidation states from +2 to +7 and can have both high-spin and low-spin states. Additionally, in nitride chemistry the unusual oxidation state +1 for manganese was recently observed in the phases $Li_2[(Li_{1-x}Mn^I_x)N]$ [21] and $Ca\{Li_2[Mn^IN]_2\}$ [22].

In this work, we present the combined N-K, Mn-$L_{2,3}$ and Ce-$M_{4,5}$, -L_3 XAS spectra of $Ce_2[MnN_3]$, CeN, η-Mn_3N_2 and θ-Mn_6N_{5+x} in order to obtain information on the electronic states of both Mn and Ce in the ternary nitride. The crystal structure of $Ce_2[MnN_3]$ contains quasi-one-dimensional Mn–N chains formed by vertex sharing of nearly square planar MnN_4 units, resulting in chains ${}^1_\infty[MnN_2N_{2/2}]$. These are three-dimensionally connected via cerium atoms. $Ce_2[MnN_3]$ is a metallic conductor and exhibits no localized magnetic moments in the susceptibility; that is, it is Pauli paramagnetic with $\chi = 4.05(2) \times 10^{-7}$ emu/g (1.53×10^{-4} emu/mol) [12]. η-Mn_3N_2 and θ-Mn_6N_{5+x} crystallize in tetragonal distorted rocksalt structures. In the crystal structure of η-Mn_3N_2 [23], the nitrogen species occupy 2/3 of the octahedral sites in an ordered way, while they are statistically disordered in the crystal structure of θ-Mn_6N_{5+x} [24]. Both η-Mn_3N_2 and θ-Mn_6N_{5+x} order antiferromagnetically below 660 K (θ-Mn_6N_{5+x}) and 913 K (η-Mn_3N_2) and have small, nearly temperature-independent magnetic susceptibilities below ambient temperatures with $\chi = 10.4–10.8 \times 10^{-6}$ emu/g ($\cong 7.0 \times 10^{-4}$ emu/mol Mn) and $\chi = 7.0–8.0 \times 10^{-6}$ emu/g ($\cong 4.8 \times 10^{-4}$ emu/mol Mn), respectively [25]. The local magnetic moments of the different crystallographic sites of manganese were determined to range from 3.3 to 3.8 μ_B by neutron diffraction [24].

2. Experimental details

$Ce_2[MnN_3]$ was prepared from CeN, manganese and nitrogen as described in Ref. [12]. CeN, η-Mn_3N_2 and θ-Mn_6N_{5+x} were prepared as spectroscopic reference materials. η-Mn_3N_2 was obtained from manganese powder and sodium azide at 750 °C, θ-Mn_6N_{5+x} ($x = 0.26$) from manganese powder and ammonia [24]. The quality of the samples was checked using X-ray powder diffraction and elemental analysis as given in Ref. [24].

The Ce-L_3 XAS spectra of polycrystalline $Ce_2[MnN_3]$ were recorded in transmission geometry at the EXAFS-II beamline of HASYLAB/DESY in Hamburg, using a Si(111) double-crystal monochromator. This resulted in an experimental resolution of ≅1.5 eV (FWHM) at the Ce-L_3 threshold (5720 eV). Due to its slight sensitivity against moist air, the sample of $Ce_2[MnN_3]$ was encapsulated in vacuum-tight stainless-steel containers, sealed by an In-metal wire, and equipped with 0.5-mm-thick Be windows. Homogeneous absorbers were prepared by grinding the studied material together with dry B_4C powder.

The Ce-$M_{4,5}$, and Mn-$L_{2,3}$ XAS measurements were recorded in total electron-yield and the N-K XAS measurements in fluorescence yield at the SX700/II monochromator operated by the Freie Universität Berlin at the Berliner Elektronenspeicherring für Synchrotronstrahlung (BESSY I). The experimental resolution at the Mn-$L_{2,3}$ threshold was 0.5 eV. The samples were ground together with gold powder, pressed into pellets and than transferred from a glovebox filled with purified Ar to the experimental chamber with a base pressure of $P = 10^{-10}$ mbar. The surfaces of the pellets were cleaned in UHV by scraping with a diamond file.

3. Results and discussion

The Mn-$L_{2,3}$ XAS spectra are known to be sensitive to the electronic state, including the spin state, and to the local environment of Mn [26]. Fig. 1 shows the Mn-$L_{2,3}$ XAS spectrum of $Ce_2[MnN_3]$ together with those of MnO and η-Mn_3N_2 which serve as references of Mn^{II}, and θ-Mn_6N_{5+x} ($x = 0.26$) and $LiMnO_2$ as references of Mn^{III}. While the main peak of $Ce_2[MnN_3]$ lies at the same energy position as those of $Mn^{II}O$ and η-$Mn^{II}_3N_2$, it is shifted to lower energy by ~1.5 eV with respect to $LiMn^{III}O_2$. This shift is very similar to those observed in the TM-$L_{2,3}$ XAS spectra going from TM^{II} to TM^{III} in 3d TM systems [2,5,26] and indicates the increase in the Mn oxidation state. Therefore, the manganese should have a similar electronic state in both $Ce_2[MnN_3]$ and η-Mn_3N_2 as that in MnO, but one has to bear in mind the larger covalency in nitrides compared with oxides (see below). The multiplet structures of the Mn-$L_{2,3}$ XAS spectra of $Ce_2[MnN_3]$ and η-Mn_3N_2 are much broader than that of MnO, which originates from delocalization of the valence electrons in the metallic nitrides. Similarly, the multiplet structure of θ-Mn_6N_{5+x} is broader than that of $LiMnO_2$. The intensities of the absorption maxima of θ-Mn_6N_{5+x} are between those obtained from the Mn^{II} and Mn^{III} compounds, what can be well understood from the average oxidation state of +2.5 referring to the ideal composition Mn_6N_5, or +2.63 for $x = 0.26$, respectively. Unfortunately no spectra of Mn^I compounds for comparison purpose are known in the literature. In Fig. 1, we present the theoretical spectra as a solid line below the data points for MnO and

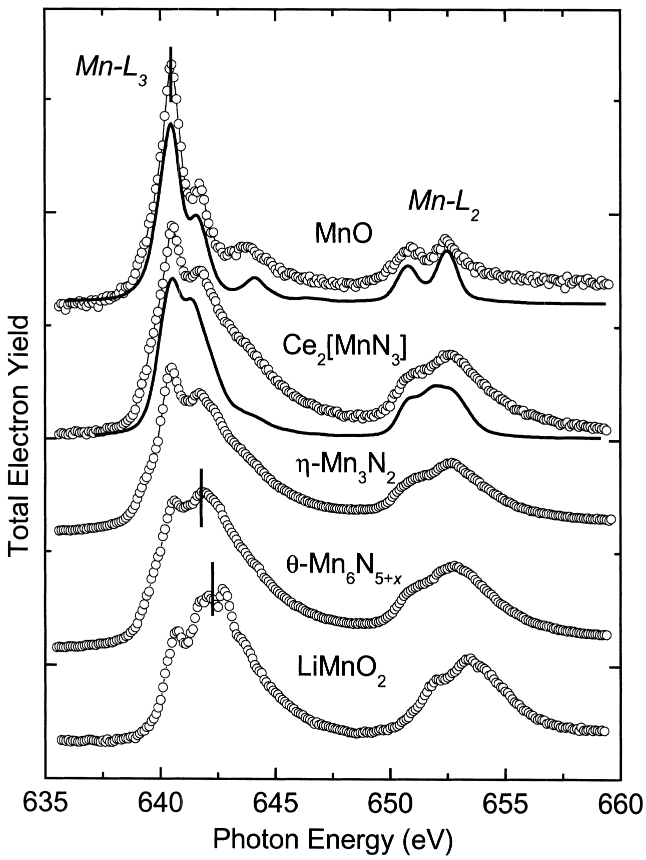

Fig. 1. Mn-$L_{2,3}$ XAS spectra of $Ce_2[MnN_3]$ together with those of η-Mn_3N_2, θ-Mn_6N_5, MnO, and $LiMnO_2$ for comparison. The solid lines below the data points for MnO and $Ce_2[MnN_3]$ represent the theoretical spectra using the crystal field multiplet calculation. The crystal field splittings 10 Dq are 0.8 eV for MnO and 0.6 eV for $Ce_2[MnN_3]$. For the latter, Ds = 0.12 eV and Dt = 0.07 eV were used (tetragonal symmetry).

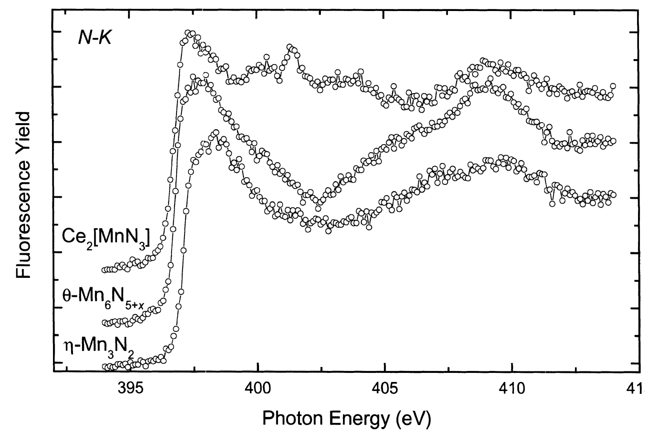

Fig. 2. N-K XAS spectra of $Ce_2[MnN_3]$, η-Mn_3N_2 and θ-Mn_6N_{5+x}.

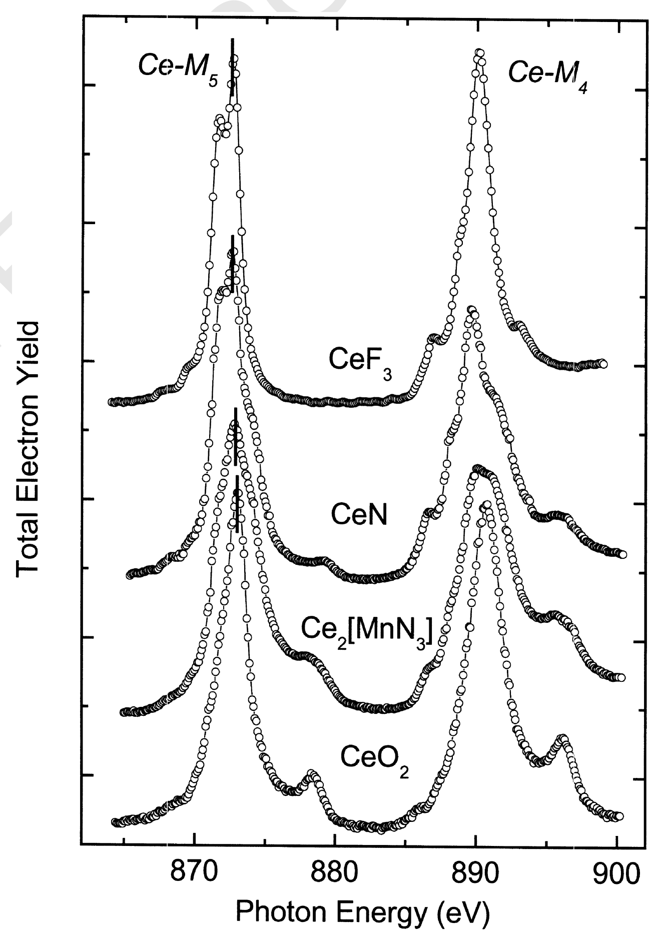

Fig. 3. Ce-$M_{4,5}$ XAS spectra of $Ce_2[MnN_3]$ together with those of CeF_3, CeN, and CeO_2 for comparison.

$Ce_2[MnN_3]$ using the crystal field multiplet calculation. The crystal field splittings 10 Dq are 0.8 eV for MnO and 0.6 eV for $Ce_2[MnN_3]$. For the latter Ds = 0.12 eV and Dt = 0.07 eV were used (tetragonal symmetry).

The branching ratio (BR) of the L_3-edge intensity to the total line strength, $I(L_3)/I(L_3 + L_2)$ [27–30], is sensitive to spin states of manganese species. The BR is found to be 0.69 for both $Ce_2[MnN_3]$ and η-Mn_3N_2 and 0.73 for MnO with a well high-spin state. The latter value is close to the theoretical value of 0.75 for the high-spin state, but much larger than 0.59 for a low-spin state obtained by theory for a $3d^5$ ion. The slightly smaller BR for η-Mn_3N_2 than for MnO would indicate an intermediate spin state as found for manganese in the magnetic spin structure of η-Mn_3N_2 [24]. For η-Mn_3N_2 and $Ce_2[MnN_3]$ nearly temperature-independent positive susceptibilities were observed. The identical BR of both phases in this study may indicate a similar Mn spin-state. Still, the branching ratios of the nitrides cannot be understood in terms of a simple ionic picture. When hybridization between Mn 3d and the conduction band occurs, the local spin at the Mn centers is suppressed. The strong delocalization of the unoccupied states can be observed in the N-K XAS spectrum; no pre-edge peak is visible. Fig. 2 compares the N-K XAS spectra of $Ce_2[MnN_3]$, η-Mn_3N_2 and θ-Mn_6N_{5+x}. Strong deviations of the branching ratios of nitridomanganates from those obtained from oxides were previously already observed [7].

Fig. 3 shows the Ce-$M_{4,5}$ XAS spectra of $Ce_2[MnN_3]$

together with those of CeF_3, CeN, and CeO_2 for comparison. Since rare-earth (RE) 4f electrons are more localized than TM-3d electrons the multiplet structures in the RE-$M_{4,5}$ XAS spectra of RE^{II} and RE^{III} compounds are scarcely affected by the local environment. The appearance of RE^{IV} spectral features depends on the degree of covalent mixing between 4f and valence electrons. From Fig. 3, one can see that the main structure of the spectrum of CeN is very similar to that of CeF_3, therefore it is close to Ce^{III}. This result obviously disagrees with previous magnetic and XPS studies [30,31] which indicated the cerium state in CeN closer to Ce^{IV} than to Ce^{III}, but supports the results of earlier XAS investigations [32] and electronic structure calculations at the LDA level of theory. The latter study indicated that the remaining electron of the Ce^{III} species is associated with the cerium centers in 5d–4f hybrid orbitals and involved in cerium–cerium interactions [20]. The difference between CeF_3 and CeN lies in a shoulder at the travelling edge (874.4 eV) and a satellite at 879.2 eV. This satellite is a characteristic feature of Ce^{IV} as observed in CeO_2 and indicates a Ce^{IV} contribution in CeN. From Fig. 3, one can see that the spectral profile of $Ce_2[MnN_3]$ is closer to CeO_2 rather than to CeN and CeF_3. Thus, we can conclude that the electronic state of the cerium in $Ce_2[MnN_3]$ is close to that in CeO_2. The spectral weight from a Ce^{III} component as the shoulder at the leading edge of the main peak is always observed after repeated scraping of the sample surface. In order to confirm that this Ce^{III} component does not originate from surface decomposition, we turned to the surface-insensitive hard X-ray measurement at the Ce-L_3 threshold (Fig. 4).

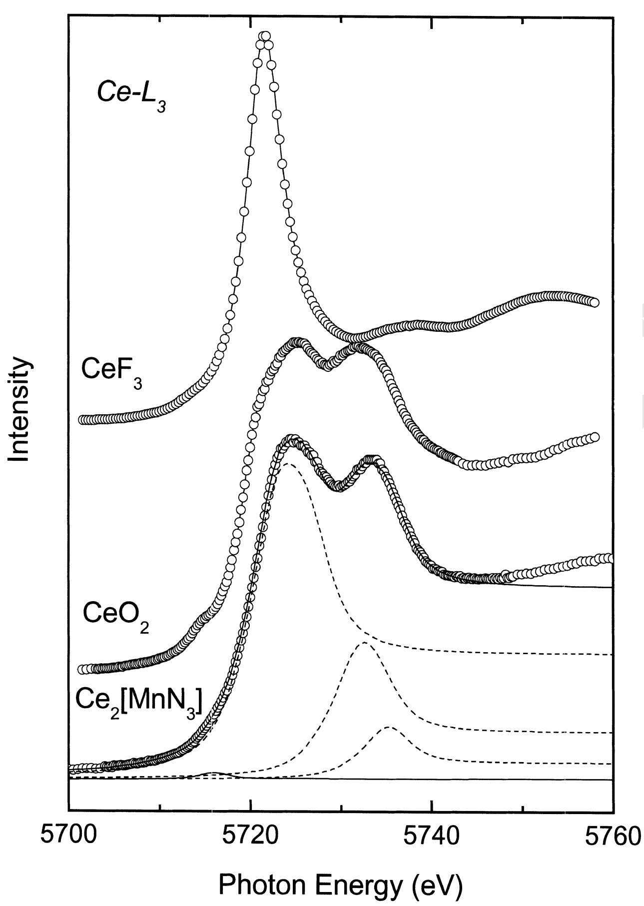

Fig. 4. Ce-L_3 XAS spectra of $Ce_2[MnN_3]$ together with those of CeF_3 and CeO_2 for comparison. The solid line through the data points of the $Ce_2[MnN_3]$ spectrum is the theoretical result consisting of three components (dashed lines, further explanation see text).

Unlike the RE^{II} and RE^{III} compounds with a single peak structure in the RE-L_3 XAS spectra, the RE-L_3 XAS spectrum of the RE^{IV} compounds shows a double-peaked structure as shown for CeO_2 due to RE-4f/ligand-2p covalence in the sense of $u_0|4f^0\rangle + v_0|4f^1\underline{L}\rangle + w_0|4f^2\underline{L}^2\rangle$ (compare Fig. 4). The observed spectral features can be well reproduced by a many-electron bonding scheme of a simplified Anderson impurity model [17]. The lower and the higher energy peak stem predominantly from $\underline{2p}4f^1\underline{L}$ and $\underline{2p}4f^0$ configurations, respectively ($\underline{2p}$ stands for the 2p core hole and $\underline{L}$ refers to the hole at the valence band). From CeO_2 to $Ce_2[MnN_3]$, the spectral weight of the lower energy peak increases by 10% indicating a decrease in the oxidation state, or, in other words, an increase in the 4f occupancy. The large linewidth in the spectrum of CeO_2 is attributed to the large crystal field splitting compared with the nitrides. The spectral intensity for each eigenvalue E_f is given by[1]

$$I(E_f) = (u_f\, u_0 + v_0\, v_f + w_0 w_f)^2 \tag{1}$$

and the average 4f electron occupancy by

$$n_f = |v_0|^2 + 2|w_0|^2 \tag{2}$$

With this simple approach, the increase in the spectral weight of the lower energy peak from CeO_2 to $Ce_2[MnN_3]$ can be understood by an increase in the 4f occupancy in the ground state from $n_f = 0.49$ to 0.52 using a decrease in Δ by 0.4 eV, while the other parameters $V = 3$ eV, $U_{cf} = 12.6$ eV, $U_{ff} = 9.5$ eV, and $U_{cd} \approx U_{fd} = 4.5$ eV stay nearly the

[1] The Hamiltonian and wavefunction in the ground state and the final state are given by the following equations:

$$\begin{pmatrix} 0 & V & 0 \\ V & U_1 & \sqrt{2}V \\ 0 & \sqrt{2}V & U_2 \end{pmatrix} \begin{pmatrix} u_f \\ v_f \\ w_f \end{pmatrix} = E_f \begin{pmatrix} u_f \\ v_f \\ w_f \end{pmatrix} \tag{3}$$

$$|\Phi_g \geq u_0|4f^0\rangle + v_0|4f^1\underline{L}\rangle + w_0|4f^2\underline{L}\rangle \tag{4}$$

$$|\Phi_f \geq u_f|\underline{2p}4f^0 5d^*\rangle + v_f|\underline{2p}4f^1\underline{L}5d^*\rangle + w_f|\underline{2p}4f^2\underline{L}^2 5d^*\rangle\ (f = 1, 2, 3) \tag{5}$$

Here $f = 0$, $U_1 = \Delta$, and $U_2 = \Delta + U_{ff}$ for the ground state, and $f = 1, 2, 3$, $U_1 = \Delta - U_{cf} + U_{fd}$, and $U_2 = 2U_1 + U_{ff}$ for the final state. Δ denotes the charge transfer energy and the parameter V represents the hybridization between the RE-4f and ligand-2p. U_{ff} is the 4f/4f Coulomb interaction, while U_{cf} and U_{fd} denote the 2p core-hole/4f and 4f/5d Coulomb interaction, respectively.

same. These results show that the cerium can be described as Ce^{IV} with a small occupation of a band mostly f in character by approximately 0.2 electrons per two Ce centers, as earlier was indicated from measurements of the magnetic susceptibility [12]. Calculations on the DFT level of theory also resulted in states immediately below the Fermi level that contain reasonably sized contributions from Ce 4f and Ce 5d orbitals [20].

4. Conclusion

The results indicate that the electronic states of the metal species in ternary rare earth-metal compounds are more complicated than expected from the oxidation states if the RE-4f electrons take part in bonding or if there is 4f covalence. In $Ce_2[MnN_3]$, the oxidation state of manganese is found to be close to that in η-Mn_3N_2, rather than in θ-Mn_6N_5 or $LiMnO_2$. The cerium 4f occupancy is about 0.52 versus 0.49 for CeO_2. Therefore, the valence state is slightly lower than 4 usually called for CeO_2. The main difficulty in interpreting the obtained spectra of manganese with respect to the electronic and the spin state is the absence of any manganese(I) spectra in the literature for comparison purposes. With advancing preparative techniques, and thus, increasing knowledge on low valency transition metal compounds, we suggest collecting a broader base of spectroscopic data.

Acknowledgements

We acknowledge financial support by the Deutsche Forschungsgemeinschaft (Fi-439/7-1 and SFB 463 'Seltenerd-Übergangsmetallverbindungen: Struktur, Magnetismus und Transport'). RN would like to thank Professor R. Kniep, Dr Yu. Grin, Dr F.R. Wagner and Professor R. Dronskowski for valuable discussions.

References

[1] J.G. Bednorz, K.A. Müller, Z. Phys. B 64 (1986) 189.
[2] Z. Hu, C. Mazumdar, G. Kaindl, F.M.F. de Groot, S.A. Warda, D. Reinen, Chem. Phys. Lett. 297 (1998) 321.
[3] C.T. Chen, L.H. Tjeng, J. Kwo, H.L. Kao, P. Rudolf, F. Sette, R.M. Fleming, Phys. Rev. Lett. 68 (1992) 2543.
[4] T. Mizokawa, H. Namatame, A. Fujimori, K. Akeyama, H. Kondoh, H. Kurada, N. Kosugi, Phys. Rev. Lett. 67 (1991) 1638.
[5] Z. Hu, M.S. Golden, J. Fink, G. Kaindl, S.A. Warda, D. Reinen, P. Mahadevan, D.D. Sarma, Phys. Rev. B 61 (2000) 3739.
[6] S. Suzuki, T. Shodai, J. Yamaki, J. Phys. Chem. Solids 59 (1998) 331.
[7] S. Suzuki, T. Shodai, Solid State Ionics 116 (1999) 1.
[8] T. Shodai, Y. Sakurai, T. Suzuki, Solid State Ionics 122 (1999) 85.
[9] R. Niewa, H. Jacobs, Chem. Rev. 96 (1996) 2053.
[10] R. Kniep, Pure Appl. Chem. 69 (1997) 185.
[11] R. Niewa, F.J. DiSalvo, Chem. Mater. 10 (1998) 2733.
[12] R. Niewa, G.V. Vajenine, F.J. DiSalvo, H. Luo, W.B. Yelon, Z. Naturforsch. 53b (1998) 63.
[13] O. Vogt, K. Mattenberger, in: K.A. GschneidnerJr., L. Eyring, G.H. Lander, G.R. Choppin (Eds.), Handbook on the Physics and Chemistry of Rare Earth, Vol. 17, Elsevier, New York, 1993, p. 301.
[14] R.D. Parks (Ed.), Valence Instabilities and Related Narrow-Band Phenomena, Plenum Press, New York, 1997.
[15] P. Wachter, H. Boppart (Eds.), Valence Instabilities, North-Holland, Amsterdam, 1982.
[16] A. Kotani, H. Mizuta, T. Jo, J.C. Parlebas, Solid State Commun. 53 (1985) 805.
[17] G. Kaindl, G.K. Wertheim, G. Schmiester, E.V. Sampathkumaran, Phys. Rev. Lett. 58 (1987) 606.
[18] Z. Hu, G. Kaindl, B.G. Müller, J. Alloys Comp. 246 (1997) 177.
[19] D.D. Sarma, O. Strebel, C.T. Simmons, U. Neukirch, G. Kaindl, R. Hoppe, H.P. Müller, Phys. Rev. B 37 (1998) 9784.
[20] G.A. Landrum, R. Dronskowski, R. Niewa, F.J. DiSalvo, Chem. Eur. J. 5 (1999) 515.
[21] J. Klatyk, R. Kniep, Z. Kristallogr. NCS 214 (1999) 445.
[22] J. Klatyk, R. Niewa, R. Kniep, Z. Naturforsch. 55b (2000) 988.
[23] H. Jacobs, C. Stüve, J. Less-Common Met. 96 (1984) 323.
[24] A. Leineweber, R. Niewa, H. Jacobs, W. Kockelmann, J. Mater. Chem. 10 (2000) 2827.
[25] M. Tabuchi, M. Takahashi, F. Kanamaru, J. Alloys Comp. 210 (1994) 143.
[26] S.P. Cramer, F.M.F. DeGroot, Y. Ma, C.T. Chen, F. Sette, C.A. Kipke, D.M. Eichhorn, M.K. Chan, W.H. Armstrong, E. Libby, G. Christou, S. Brooker, V. McKee, C. Mullins, J.C. Fuggle, J. Am. Chem. Soc. 113 (1991) 7937.
[27] B.T. Thole, G. van der Laan, Phys. Rev. B 38 (1988) 3158.
[28] T.G. Sparrow, B.G. Williams, P. Bezdicka, L. Fournes, A. Wattiaux, J.C. Grenier, M. Pouchard, Solid State Commun. 91 (1994) 501.
[29] R.D. Leapman, L.A. Grunes, P.L. Fejes, Phys. Rev. B 26 (1982) 614.
[30] Y. Baer, R. Haugger, Ch. Zürcher, M. Campagner, G.K. Wertheim, Phys. Rev. B 18 (1978) 4433.
[31] D.W. Lynch, J.H. Weaver, in: K.A. GschneidnerJr., L. Eyring, S. Hüfner (Eds.), Handbook on the Physics and Chemistry of Rare Earths, Vol. 10, Elsevier, New York, 1987, p. 231.
[32] J.P. Kappler, E. Beaurepaire, G. Krill, J. Serenis, C. Godart, G. Olcese, J. Phys. I, Fr. 1 (1991) 1381.